Photometric Observations of a Very Young Family-Member Asteroid (832) Karin

Fumi Yoshida[1] Budi Dermawan[2,3] Takashi Ito[4] Yu Sawabe[5] Masashige Haji[5]
Ryoko Saito[5] Masanori Hirai[5] Tsuko Nakamura[1] Yusuke Sato[6]
Toshifumi Yanagisawa[7] and Renu Malhotra[4]

[1]*National Astronomical Observatory of Japan, Osawa, Mitaka, Tokyo, 181-8588, Japan*
yoshdafm@cc.nao.ac.jp

[2]*School of Science, University of Tokyo, Bunkyo, Tokyo 113-0033*

[3]*Department of Astronomy, Bandung Institute of Technology, Bandung 40132, Indonesia*

[4]*Lunar & Planetary Laboratory, The University of Arizona, Tucson, AZ 85721, USA*

[5]*Dept. Earth Sciences & Astronomy, Fukuoka University of Education,*
1-1, Akama-Bunkyo-machi, Munakata-shi, Fukuoka, 811-4192, Japan

[6]*Department of Astronomy, University of Tokyo*

[7]*Japan Aerospace Exploration Agency, Institute of Space Technology and Aeronautics,*
7-44-1, Jindaiji-higashi-machi Chofu-shi, Tokyo, 182-8522, Japan

(Received 2004 March 15; accepted 2004 April 15)

Abstract

Asteroid (832) Karin is the largest member of the Karin family which was recently identified and estimated to be 5.8 Myr old by Nesvorný *et al.* (2002) with a sophisticated numerical integration technique. The Karin family is regarded as an outcome of a collision in such recent times. In order to make clear the physical aspect of this family-forming event, we performed photometric observations of Karin from July to September, 2003. We report here its lightcurve and colors in optical bands. The rotational period of asteroid Karin was determined to be 18.346 ± 0.096 hr. Its absolute magnitude (H) and the slope parameter (G) of the phase curve at R-band are 11.49 ± 0.02 and 0.19 ± 0.04, respectively. Based on our color observations, we confirmed that this asteroid belongs to the S-type asteroid group. Moreover, we probably found that there is a color variation over the surface of Karin. We infer that the color variation is due to the difference between the fresh surface excavated by the family-forming disruption and the weathered surface exposed to the space radiation and particle bombardment for a long time.

Key words: Solar system:Asteroids:Minor planets:Lightcurve:Colors:Photometry

1. Introduction

The young Karin family was discovered by Nesvorný *et al.* (2002). This family was estimated to be formed 5.8 ± 0.2 Myr ago. It consists of 39 asteroids with a size range from about 1.5 km to 20 km in diameter. Most of asteroid families are considered to be very old (~ 2 Gyr), and to have undergone significant collisional and dynamical evolutions since their formation. Such evolutions must have masked the properties of the original collision. However, the age of the Karin family is estimated to be remarkably young by numerical integrations of orbits. Therefore it is likely that the members of the Karin family still preserve some aftermath of the original collisional event which formed the family.

The Karin family called our attention to the following three aspects: (1) the tumbling (wobbling) motion of each family member; i.e. non-principal axis rotation of the asteroids, (2) the spin period and the shape distributions of the family members, and (3) the color variation on the asteroids' surface or between the members.

As for (1), the tumbling motion of the solar system small bodies has so far been confirmed only for the comet Halley and some asteroids (e.g. Mueller *et al.*, 2002). Study of the tumbling motion gives us important insights into the energy dissipation inside a celestial body. Regarding asteroids, the tumbling motion could be excited by collisions of small projectiles, and it is damped by the internal energy dissipation. If the damping timescale of the tumbling motion after a collisional event is long enough, we may be able to observe it even now (asteroid (4179) Toutatis is a good example as such). If an asteroid is in a state of the tumbling motion, it should appear in its lightcurve as the multiple periods.

As for (2), very little is known so far about the rotational states of asteroid families as fragments just after a catastrophic disruption that created them. According to Rubincam (2000), the Yarkovsky-O'Keefe-Radzievskii-Paddack (YORP) effect may spin up or spin down 10-km diameter asteroids on a 10^8-year timescale, whereas smaller asteroids could spin up or down even faster. Therefore, in the case of old asteroids, the YORP effect may have changed the initial spin rate after a collision. However, since the Karin family is significantly younger than the timescale of the YORP effect, each member could still keep its initial spin rate. The rotational period distribution of the members of a family reflects the angular momentum distribution of the fragments from a disruption event. This could be one of the primary clues to know the detailed condition of the breakup event forming an asteroid family.

The shape distribution of the family-forming asteroids is also important. If an asteroid has a very elongated shape, it must be a monolithic asteroid or a binary asteroid. Meanwhile, if an asteroid of a considerable size is spherical, it is likely to be a rubble-pile asteroid, which consists of several or many small reaccumulated fragments due to gravity. The shape distribution of the Karin family asteroids would thus allow us to give valuable information on the fragmentation process caused by a large disruption event of celestial bodies. In this respect, we

would say that the observation of the Karin family asteroids gives us the first and also unique opportunity to compare results of the laboratory experiments of the collision with the ones from an actual collision between celestial bodies.

About the aspect (3), asteroid (832) Karin has been known that it is a S-type asteroid (Binzel, 1987). The spectra of S-type asteroids are believed to have changed by the "space weathering" (e.g. Sasaki *et al.*, 2001). It predicts that the slope of spectra of the mature surface exposed to the space for a longer time is steeper at the optical-band region and the 1μm-band absorption depth in the spectra becomes lower by optical maturation processes. So the different surface properties can be detectable by the photometry or spectroscopy if it exists. Given that Karin is a remnant from a catastrophic disruption, it is likely that Karin has both an old surface exposed to the space for a long time and a fresh surface excavated by the family forming collision. Such an example of surface heterogeneity has been reported for asteroid (433) Eros (Sullivan *et al.*, 2003), whose surface was composed of the mature part covered by a thick regolith layer and the fresh part made of the internal material which was probably exposed by seismic vibration of impact events.

Generally, the members of one asteroid family have the same taxonomic type, because they were formed from one parent body. So it is reasonable for us to assume that the Karin family is a cluster consisting of S-type asteroids. If the time scale that the space weathering completely changes optical properties on the asteroid surface is longer than the age of the Karin family, we may find the different colors among members of the Karin family; namely the fragment chips coming from inside of the parent body will show original fresh colors, whereas the ones from the surface of the parent body have matured colors.

Based on the three motivations described above, we began to observe the lightcurves of each member of the Karin family from 2002 November. In this paper, we report the results of the lightcurve and color observation of Karin. In section 2, we mention our observations. Section 3 deals with the lightcurve analysis and the determinations of the rotation period, the absolute magnitude, the slope parameter, and the size and shape of Karin. We describe in section 4 the results of the color observation. There, the taxonomic type of Karin and the color variation on the surface are analyzed. In section 5, we summarize the results of our observations, with some discussion.

2. Observations

The observations of Karin were performed from 2003 July to September. We used three telescopes; the Vatican Advanced Technology Telescope, which is the 1.8 m telescope at the Vatican observatory (Mt. Graham, Arizona, USA), the 1-m Schmidt telescope at the Kiso observatory (Japan), the 40-cm telescope at the Fukuoka University of Education (Japan). The locations of telescopes and the instruments are listed in table 1.

We usually used the R-filter, because the R-filter is most efficient at the peak intensity

of the solar spectra. At the Fukuoka University of Education, we used the Fuji filter (SC60) made by Fuji-film co., which has a similar property to the R-filter, because they didn't have a R-filter. The telescopes were driven at a sidereal tracking rate. Therefore, the exposure time is limited by the motion of the asteroid and by the seeing size at the observing nights. We chose exposure times of $40 \sim 100$ sec so that the asteroid looks like a point source. The R-band-imaging was continued consecutively all through the nights. The B, V, R, I-band-observations were carried out at the Vatican Advanced Technology Telescope on 2003 September $26 \sim 29$ (UT). The several Landolt photometric standard stars (Landolt, 1992) were also observed a few times (whenever possible) at each band on each night. Before and/or after each observation, we took several dome flat or twilight sky flat images for flat-fielding.

All data were reduced with the standard procedures using the IRAF: the bias or dark image was subtracted from each image and then the frame was divided by the median-flat-image. Next the aperture photometry was performed with the APPHOT package of the IRAF. In the lightcurve observation, the asteroid brightness was measured relative to the field stars on the same frame that were listed in the USNO-2 catalog. As for the color observation (we will explain more in detail in section 4), we made the extinction curve at each band, and corrected the brightness of the asteroid with it.

Table 2 shows the summary of Karin's observation log and ephemeris. The first column is the date and time referred to the mid-time of each observing night. The next two columns are the RA and DEC of the asteroid at the time of the first column. The fourth and fifth columns are the distances of the asteroid from the Sun and the Earth, respectively. The next column is the solar phase angle. Column 7 shows the sky motion of the asteroid. The names of the observatories are listed in the last column. We chose only the high quality data from table 2, namely August 22-23, September 3-5 and 26-29 covering consecutive nights, and used them in the analysis of the following section.

3. Lightcurves of Karin

3.1. Zero-level correction

We took the data from different telescopes with different instruments, so we need a careful calibration when combining multiple observing runs. At first, we derived the rough rotational periods of Karin separately for each lightcurve data of the consecutive nights. In determining its rotational period, we employed the following two different methods. One is the Lomb's Spectral Analysis (SpAn) (Lomb, 1976) and another is the WindowCLEAN analysis which incorporates a discrete Fourier transform and the CLEAN algorithm (Robert *et al.*, 1987). We accepted the periods detected with the highest probability in both methods. And then we used the following sequence proposed by Harris & Lupishko (1989) to construct the synthesized lightcurve (Dermawan *et al.*, 2002). The synthesized lightcurve was calculated by

changing the fitting order of the Fourier series in equation (1) up to the 8th ($j = 8$) order for each observing run, to search for the best fit value of j.

The Fourier series for out fitting purpose is given as follows:

$$H(\alpha,t) = \bar{H}(\alpha) + \sum_{i=1}^{j}\left[A_i \sin\frac{2\pi i}{P}(t-t_0) + B_i \cos\frac{2\pi i}{P}(t-t_0)\right] \quad (1)$$

where $H(\alpha,t)$ is the reduced magnitude at the solar phase angle α at the time t. $H(\alpha,t)$ is expressed by $H(\alpha,t) = m(\alpha,t) - 5logR\Delta$, in which $m(\alpha,t)$ is the apparent magnitude, R is the distance between Sun and asteroid, and Δ is the distance between Earth and asteroid, respectively. $\bar{H}(\alpha)$ is the average of the $H(\alpha,t)$ in each observing run, P the period which was determined by the analysis of periodicity, j the order of equation (1), and t_0 the epoch of time. The constant component of thus obtained best-fitted curve is equivalent to the zero-level magnitude at each observing run. Then we combined the lightcurves of multiple observing runs based on those zero-levels. We got eventually the lightcurve of Karin from observations covering over more than one month. After that, we conducted a period analysis again for the long-term lightcurve data and determined the final rotational period. For testing the "goodness of fit", the following χ^2 value was also calculated:

$$\chi^2 = \sum_{l=1}^{N}\left[\frac{H_l - H(\alpha,t)}{\sigma_l}\right]^2, \quad (2)$$

where H_l and $\sigma_l$are the observed magnitude and its error, respectively, N is the number of data, and $H(\alpha,t)$ is the synthesized magnitude obtained from equation (1), The above described process to examine the periodicity of the lightcurves was repeated several times until the result converges to the best-fit synthesized lightcurve.

3.2. Rotational period of Karin

Figure 1 shows the results of the period analysis applied to the final lightcurve obtained in section 3.1 which was calculated by the SpAn and the WindowCLEAN methods. Both the methods detected the very consistent period of 0.7645 day for the lightcurve with a high probability. Except the periods for the daily aliases and the sub- or higher harmonics, some other independent periodicities were also detected with low confidence. We checked those periodicities in the rotational phased data. However, since they did not give any appreciable changes in lightcurves, Karin is unlikely to be in a state of multiple-period rotation, which is a necessary symptom of the tumbling motion (Muller *et al.* 2002). We determined the rotational period of the Karin to be 0.7645 ± 0.0040 day (18.348 ± 0.096 hr). The synthesized lightcurve with this period was shown in figure 2.

In 1984, Binzel (1987) already observed the lightcurve of this objects, with the obtained period of 18.82 hr. However, since the time interval covered by his observations was only two days, we believe that our period is much more reliable and robust.

3.3. *Lightcurve amplitude*

It has long been known that the light variation of an asteroid is subject to change as a function of the solar phase angle. Zappala *et al.* (1990) found how the lightcurve amplitude of an asteroid depends on the solar phase angle at which the asteroid was observed. Since we observed Karin at different solar phase angles in multiple observing runs, the amplitude of each lightcurve obtained in each observing run must be different. So we calculated for normalization the amplitude at zero phase angle by the following empirical correction which was proposed by Zappala *et al.* (1990):

$$A(0^\circ) = A(\alpha)/(1 + m\alpha), \tag{3}$$

where $A(0^\circ)$ and $A(\alpha)$ are the lightcurve amplitude at the zero solar phase angle and the one at the phase angle of α. Parameter m is empirically known to be 0.030, 0.015, and 0.013 degree^{-1} for S-, C-, M-type asteroids, respectively. We used $m = 0.030$ here, because Karin is a S-type asteroid (Binzel 1987, and see section 4 in this paper). Thus we obtained that the peak-to-peak amplitude of the lightcurve is 0.68 ± 0.02 magnitude at the zero solar phase angle. On the other hand, Binzel (1987) found in his observation of 1984 that the peak-to-peak amplitude was 0.32 magnitude. Because the difference Binzel's amplitude and ours observed at different aspect angles is surely significant in statistical sense, both the data will be used for future determination of the spin pole orientation and the true shape.

When the asteroid's shape is approximated to be a triaxial ellipsoid and it is assumed that the asteroid was observed at the aspect angle of 90° (aspect angle: the angle between the line of sight and the rotation axis), the above amplitude corresponds to the axis ratio a/b as follows.

$$\log_{10}(a/b) = 0.4A(0^\circ), \tag{4}$$

where $A(0^\circ)$ is the amplitude at the zero phase angle. So from this relation, we obtain that the ratio a/b is 1.91. Since we do not know the direction of the rotation axis of Karin, this value is actually a lower limit to the intrinsic axis ratio. In any case, Karin seems to have an elongate shape.

3.4. *Phase curves and size of Karin*

Since we observed Karin with the range of the solar phase angles between 0.6 and 14.3 degrees, we could also get its phase curve (see figure 3). We calculated the mean magnitudes of Karin by reducing the heliocentric and geocentric distances to unity in each consecutive observing run, and plotted them as a function of the solar phase angle in figure 3. The error bars of each data point are the mean error measured for each observing run. Then the phase curve of Karin was fitted using the $H - G$ magnitude system approved by the IAU (Bowell *et al.*, 1989), which contains two free parameters: its absolute magnitude (H) and slope parameter (G). The $H - G$-magnitude system connects the reduced magnitude of an asteroid ($H(\alpha)$) to

the absolute magnitude, as follows,

$$H(\alpha) = H - 2.5\log[(1-G)\Phi_1(\alpha) + G\Phi_2(\alpha)], \quad (5)$$

where $\Phi_1(\alpha)$ and $\Phi_2(\alpha)$ are the given functions of the phase angle. The thus fitted curve is shown by the solid curve in figure 3. Our best estimated absolute magnitude H_R is 11.03 ± 0.02 mag for R-band and the slope parameter G_R is 0.19 ± 0.04. We discuss in section 4 H and G values corresponding to V-band.

4. Color observation of Karin

4.1. Relative reflectance and shape of Karin

We conducted the $BVIR$-color observations of Karin with the VATT2K CCD attached to the 1.8 m Vatican Advanced Technology Telescope of the Vatican observatory on 2003 September 26-29 (UT). We used B, V, R, and I-filters, whose bands are centered at 4359.32, 5394.84, 6338.14 and 8104.87 $\mathring{A}$, respectively. For photometric calibration, we observed a few Landolt standard stars (Landolt 1992) with each filter on every night, and then determined the extinction coefficients for B, V, R, and I-bands under the standard reduction procedure. The photometric reduction and the aperture photometry were performed using the IRAF and its APPHOT package, as we did for lightcurve observations. The magnitude of asteroids observed at different airmasses were corrected by using the extinction coefficients of each band. In order to remove the effect of the magnitude variation due to the asteroid's rotation which affects asteroid colors, we always took R-band data just before and after we observed with different filters, so our observing sequence is like this; $RR-BB-RR-II-RR-VV-RR$.... This observation and results are listed in table 3.

As one can see in figure 4, we got the color data for the almost whole range of the rotational phase of Karin, i.e. phase 0 to 0.9. At first, we calculated the average colors for the entire surface of Karin as: $B-V = 0.783 \pm 0.014$, $V-R = 0.452 \pm 0.002$, $V-I = 0.831 \pm 0.018$.

Then we plotted Karin's colors on the two-color diagrams (see figures 5, the red dots with error bars show the Karin). For comparison, we also plotted in figure 5 the S, C, D, and M-type asteroids taken from Zellner *et al.* (1985). According to Binzel's observation (1987), Karin belongs to a S-type asteroid. In our result on the other hand, one can see that Karin lies near the edge of S-type group in figures 5. Therefore, we confirmed that Krain is of S-type.

Next, by subtracting the solar colors ($B-V = 0.665$, $V-R = 0.367$, $V-I = 0.705$) (Rabinowitz, 1998) from Karin's colors, we obtained the relative reflectance of Karin as a function of the wavelength and showed it in figure 6 with red circles with error bars. Note that the error bars are hiding behind the circles, because they are very small. The relative reflectances of the other S-type asteroids, which we got from the "Small bodies Node" of the small bodies data base (http://pdssbn.astro.umd.edu/, EAR-A-DBP-3-RDR-24COLOR-V2.0, Asteroid 24-Color Survey), are shown with cross marks in the same figure. The relative

reflectance of each asteroid was normalized at the wavelength of 0.56 μm. Though the relative reflectance of Karin is confined within the spectral variation of the other S-type asteroids, it seems to be somewhat flatter than the ones of the other S-type asteroids.

Since the mean colors of Karin have been obtained above, we are now in a position to calculate the H and G in V-band of this asteroid and the corresponding diameter. First, we converted each H_R in figure 3 to H (in V-band) using Karin's color and refitting those data with H-G equation (5). As a result, we got $H = 11.49$. As for G, we assume here that $G = G_R$. Bowell *et al.* (1989) gave a relation connecting the diameter D(km) with H as:

$$logD = 3.130 - 0.5logp - 0.2H. \tag{6}$$

where p is the albedo. Since we know that Karin is a S-type asteroid, we assume that $p = 0.20$ for this object (corresponds to the mean value of the albedo for the S-type asteroids from the PDS data set IRAS-A-FPA-3-RDR-IMPS-V4.0:http://www.psi.edu/pds/archive/albedo.html). Then, with equation (6), one can estimate the diameter of Karin as $D = 15.3 \pm 0.14$ km. Furthermore, if we adopt the a/b of 1.91 for Karin as seen in the edge-on aspect (section 3.4), we can obtain 21.1×11.1 km for the ellipsoidal sizes.

4.2. Color variation on Karin's surface

We also investigated the color variation over the Karin's surface. As mentioned before, we got the color data for a wide range of the rotational phase between 0 and 0.9 (see figure 4). We hence divided the data into seven rotational phases and examined the colors; $B-V$, $V-R$, and $V-I$ at each phase. Figure 7 shows the color variation of Karin depending on the rotational phase. The $V-R$ is seen to be almost constant through all the rotational phases. The $B-V$ is small at small phases, gradually becomes large, and reaches to the maximum at around 0.6 of phase. Considering that each error of measured Karin magnitudes is less than 0.005 mag, the variation range of the $V-I$ color, ~ 0.13, seems to be very high, though the data point are not so dense. So we believe that the large variation of the $V-I$ in particular is real. These color variations suggest that Karin possesses an inhomogeneous surface.

From figure 7, the Karin's colors seems to be different roughly before and after the phase of 0.5. This may mean that Karin has different faces on each hemisphere. Therefore, we examined the relative reflectance of each hemisphere. The relative reflectances for two hemispheres are shown in figure 8. In figure 8, the black solid line represents the relative reflectance on the first hemisphere and the gray one shows that on another one. Both relative reflectance were normalized at V-band. One can notice the large relative reflectance variation especially at I-band, which in consistent with figure 7.

5. Summary and Discussion

5.1. Summary

Our observation revealed the followings:

1. The rotational period of Karin is 18.348 ± 0.096 hr. There was no clear indication of multiple-period rotation. Therefore, Karin probably does not have a tumbling motion. The lightcurve shows that the peak-to-peak range (Δm) is 0.68 ± 0.02 mag at the zero solar phase angle. If we assume an ellipsoidal body for Karin, the Δm means that the ratio $a/b = 1.91$ when projected onto the sky plane.

2. The absolute magnitude (H) is 11.49 ± 0.02 mag, and the slope parameter (G) of the phasecurve is 0.19 ± 0.04. If we assume that the albedo of Karin is $p = 0.20$ (this value correspond to the average albedo of S-type asteroids), the mean diameter of Karin becomes 15.3 ± 0.14 km, corresponding to the Karin's ellipsoidal shape of $21.1 \times 11.1 km$.

3. The average colors of the almost entire surface of Karin are: $B - V = 0.783 \pm 0.014$, $V - R = 0.452 \pm 0.002$, and $V - I = 0.831 \pm 0.018$ mag. From those colors, we confirmed that Karin belongs to the S-type asteroid group.

4. We found a color variation over the Karin's surface. We propose that the variation is due to that a variegation of young and old surfaces exists on Karin.

We are now observing other Karin family asteroids. We have observed so far twelve Karin family members except Karin. The results will be published in subsequent papers.

5.2. Discussion

Believing that Karin is a remnant of fragments from a disruption event, it is likely that Karin has both a fresh surface excavated by the family-forming disruption and the weathered surface exposed to the space radiation and particle bombardment for a long time. Can the difference of the reflectance that we found be interpreted as an optical difference between the fresh and matured surfaces?

The idea that S-type asteroids are parent bodies of ordinary chondrites seems to have been confirmed by recent evidence provided by telescopic observations (Binzel *et al.*, 1996), spacecraft NEAR-Shoemaker mission (Mcfadden *et al.*, 2001, Bell *et al.*, 2002) and laboratory experiments (Sasaki *et al.*, 2001). The mismatch of the reflectance spectra between S-type asteroids and ordinary chondrites, which was regarded as a "paradox" in the past, seems now to be explained by the effects of the space weathering growing with the surface age (Sasaki *et al.*, 2001, Clark *et al.*, 2003). Therefore, if the above mentioned scenario is correct, it is suggested that the reflectance spectra of a fresh surface of S-type asteroids are close to those of ordinary chondrites, meanwhile, the spectra of old surface show the reddened spectra which are common among S-type asteroids. Along this line of thought, Binzel *et al.* (1996) arranged the reflectance spectra in the visible wavelength region for several near-Earth asteroids, a typical

main-belt S-type asteroid, and an average H6 chondrites, as a sequence of a degree of space weathering. Given this sequence of the age, one can judge that the surface with the black solid-line spectrum (figure 8) is older than that with the gray-line spectrum. Moreover, comparison of figure 8 with the above Binzel's spectra indicates that the Karin's mature surface is younger than the average main-belt S-type asteroid and the Karin's fresh surface is older than the average H6 chondrite.

The existence of the color variation found in this observation, namely the inhomogeneity of the Karin's surface is supported by the other spectroscopic observations of Karin using the Subaru telescope (Sasaki *et al.* 2004). They used the 8.2m Subaru telescope attached with the Cooled Infrared Spectrograph and Camera for OHS (CISCO) and observed Karin with near-infrared wavelengths, zJ(0.88-1.40 μm), JH(1.06-1.82 μm), and wK(1.85-2.51 μm) on September 14, 2003 (UT). They got three spectra of Karin by three exposures. The integration time for each setting was 2400 sec. Their three spectra were obtained at phases of 0.3-0.34, 0.35-0.38 and 0.45-0.50 in figure 2. They found a significant difference on the slopes between the spectrum obtained at the first exposure and the others. The former was the spectra of S-type asteroids, while the latter two matched well with the spectra of ordinary chondrites. Therefore, they interpreted the difference of the spectra as the mixed distribution of the matured and fresh surfaces on Karin. According to Sasaki *et al.* (2004), the optical properties on the Karin's surface suddenly changed from the matured surface to the fresh one around rotational phase of 0.35. In our data, on the other hand, the matured surface appeared abruptly at phase of 0.2 and the fresh surface resumed after phase 0.3. There are no data point around phase 0.4 in our data. Although the cause of the small mismatch in phase between the spectroscopy (Sasaki *et al.*, 2004) and our photometry is unknown, both results are consistent in that Karin's surface has a heterogeneity near phase of $0.2 \sim 0.3$ consisting of the mature and fresh hemispheres.

We thank Drs. Matt Nelson, Guy Consolmagno, and Stephen Tegler for giving us a long, extensive, and formidable training for observing at VATT. We also thank Dr. Tom Gehrels for recommending us applying for VATT, and Richard Boyle who took care of our stay at Mt. Graham during our observation. The first author (Y.F.) acknowledges the financial support from the Sumitomo Foundation for the research funding 030755. Part of the data analysis was performed at Astronomical Data Analysis Computer Center, National Astronomical Observatory of Japan.

References

Bell, J. F. III *et al.* 2002, Icarus, 155,119

Binzel, R. P. 1987, Icarus, 72, 135

Binzel, R. P., Bus, S. J., Burbine, T. H., Sunshine, J. M. 1996, Science, 273, 946

Bowell, E., Hapke, B., Domingue, D., Lumme, K., Peltoniemi, J., Harris, A. W. 1989, in Asteroids II, eds Binzel, R. P., Gehrels, T., Matthews, M. S., (The University of Arizona Press, Tucson, Arizona) 331

Clark, B. E., Hapke, B., Pieter, C., Britt, D. 2003, in Asteroids III, eds Bottke, W. F. Jr., Cellino, A., Paolicchi, P., and Binzel, R. P. (The University of Arizona Press, Tucson, Arizona) 585

Dermawan, B., Nakamura, T., Fukushima, H., Sato, H., Yoshida, F., Sato, Y. 2002, PASJ, 54, 635

Harris, A. W. & Lupishko, D. F. 1989, in Asteroids II, eds Binzel, R. P., Gehrels, T., Matthews, M. S., (The University of Arizona Press, Tucson, Arizona) 39

Landolt, A.U. 1992, AJ., 104, 340

Lomb, N. R. 1976, Astrophysics and Space Sci., 39, 447

Mcfadden, L. A. *et al.* 2001, Meteo. Planet. Sci., 36, 1711

Michel, *et al.* 2003, Nature, 421, 608

Mueller, B. E. A., Samarasinham, N.H., Belton, M. J. S. 2002, Icarus, 158, 305

Nesvorný, D., Bottke, W. F. Jr, Dones, L., Levison, H. F. 2002, Nature, 417, 720

Rabinowitz, D. L. 1998. Icarus, 134, 342

Robert, D. H., Lehar, J., Dreher, J. W. 1987, AJ, 93, 968

Rubincam, D.P. 2000. Icarus, 148, 2

Sullivan, R. J., Thomas, P. C., Murchie, S. L., Robinson, M. S. 2003, in Asteroids III, eds Bottke, W. F. Jr., Cellino, A., Paolicchi, P., and Binzel, R. P. (The University of Arizona Press, Tucson, Arizona) 331

Sasaki, S., Nakamura, T., Hamabe, Y., Kurahashi, E., Hiroi, T. 2001, Nature, 410, 555

Sasaki, T., Sasaki, S. Watanabe, J., Sekiguchi, T., Kawakita, H., Fuse, T., Takato, N., Yoshida, F., Dermawan, B., Ito, T. 2004, in preparation.

Zappala, V. *et al.* 1990, A&A, 231, 548

Zellner, B. *et al.* 1985, Icarus, 61, 355.

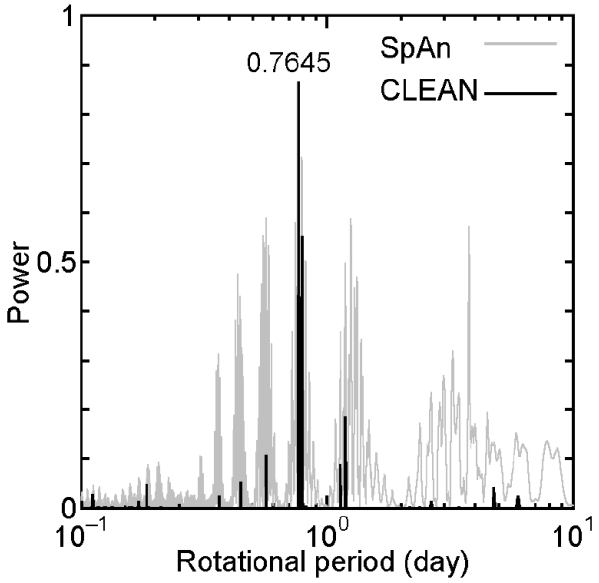

Fig. 1. Periodicities in Karin's lightcurve derived by methods of the Lomb's Spectral Analysis (SpAn) (Lomb, 1976) and WindowCLEAN based on the CLEAN algorithm (Robert *et al.*, 1987). Note that the agreement of the main peak is very good.

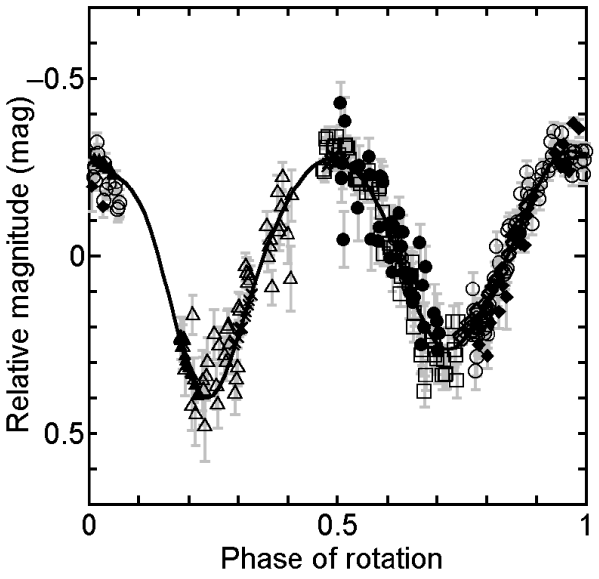

Fig. 2. Lightcurve of Karin. The rotation period is found to be 18.346 ± 0.096 hr. The peak-to-peak amplitude is 0.68 ± 0.02 mag at the zero phase angle.

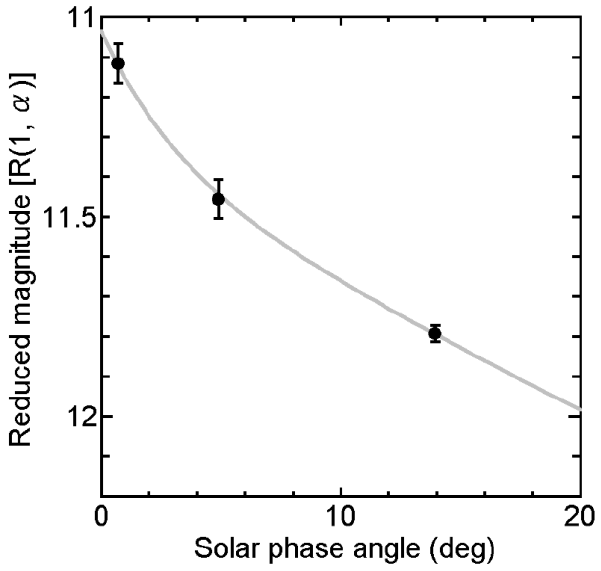

Fig. 3. Phase curve of Karin. The absolute magnitude (H_R) reduced to the zero phase angle is 11.03 ± 0.02 mag. The slope parameter (G_R) is found be 0.19 ± 0.04

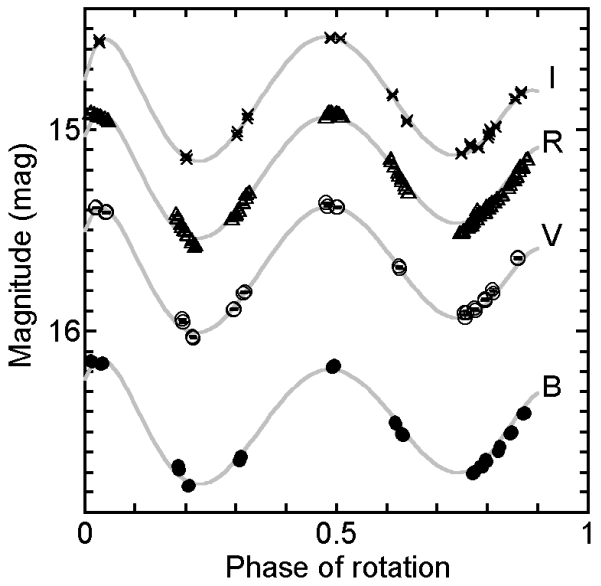

Fig. 4. Distribution of color observation plotted on the Karin's rotational phase curve. We always took the R-band images before and after we use the different filters. We observed Karin at least for a few hours in one night. There are the data sets for 2 days around phase 0.8. The phase of rotation was adjusted to the one in figure 2.

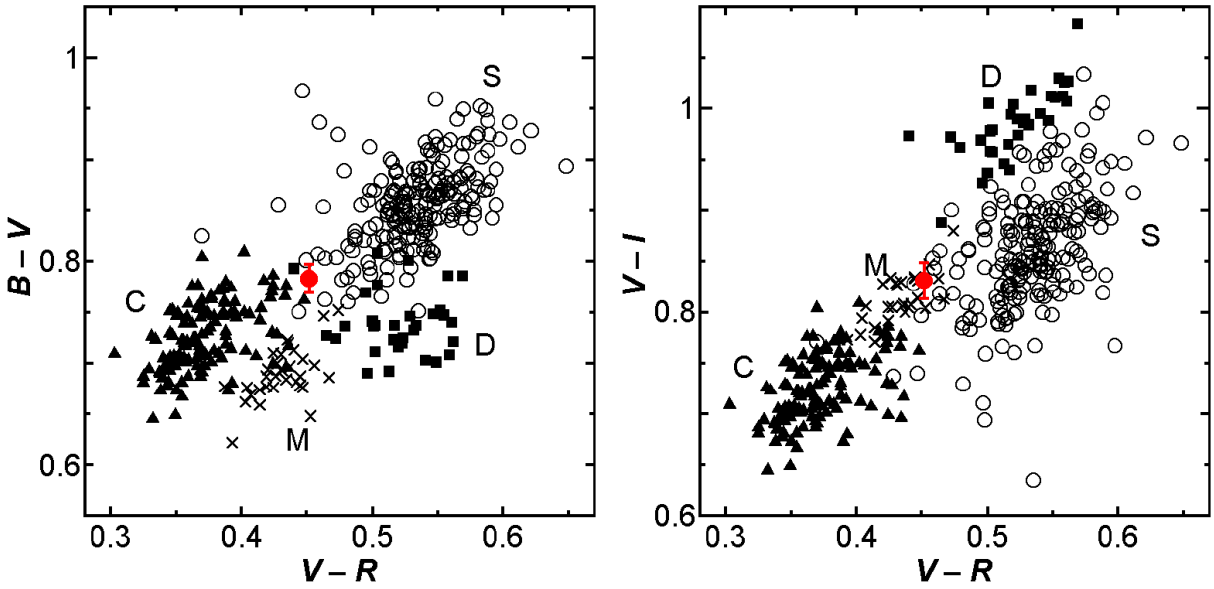

Fig. 5. Colors of Karin (with red error bars) on $V-R$ vs. $B-V$ (left) and $V-R$ vs. $V-I$ (right) diagrams. ∘, △, , and × denote S-, C-, D-, and M-type asteroids, respectively. The asteroid data are taken from Zellner *et al.* (1985).

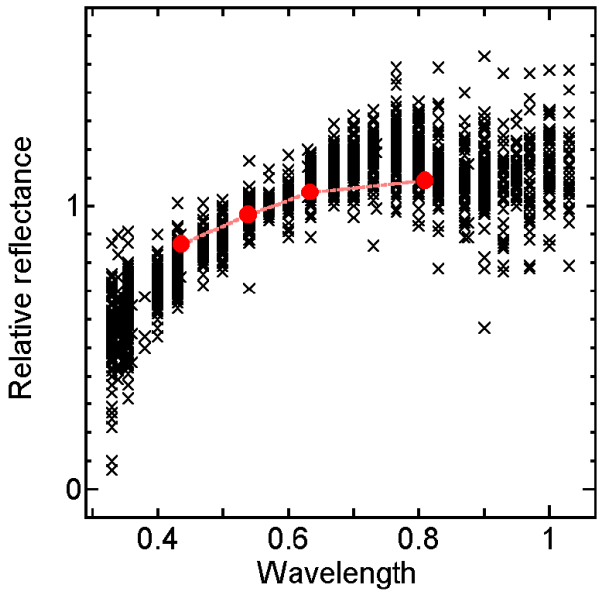

Fig. 6. Relative reflectance of Karin. After the solar colors were subtracted from Karin's colors, the relative magnitude of each band relative to V-band was calculated and then converted to the relative reflectance of the Karin (red one). × shows the relative reflectance of several S-type asteroids. The data are from the "Small bodies Node" of the small bodies data base (http://pdssbn.astro.umd.edu/, EAR-A-DBP-3-RDR-24COLOR-V2.0, Asteroid 24-Color Survey). All spectra were normalized at the wavelength of 0.57 μm.

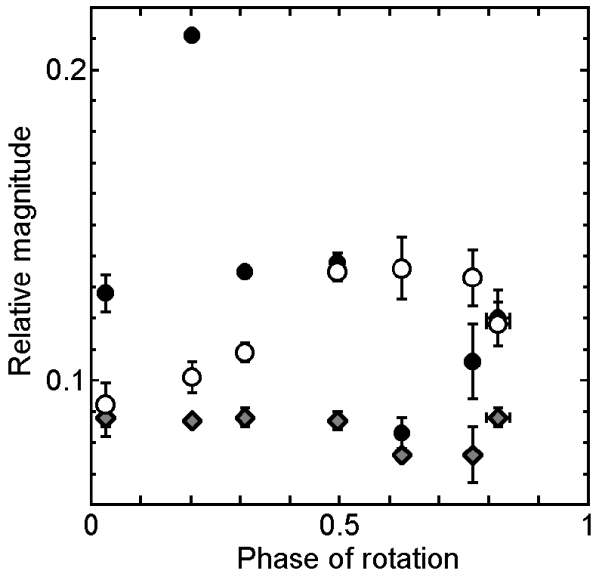

Fig. 7. Color variation on Karin's surface. ○, ◇, and • denote $B-V$, $V-R$, and $V-I$ colors, respectively. The $V-R$ remains almost constant at all the phases. The $B-V$ and $V-I$ are seen to vary at each hemisphere before and behind of 0.5 phase.

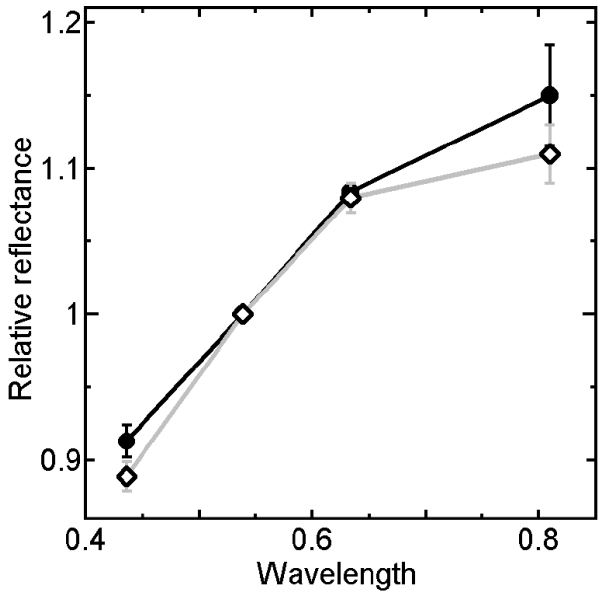

Fig. 8. Relative reflectance at the different hemispheres of Karin. The black solid line shows the relative reflectance at the first half of the hemisphere and the gray one shows that of another half. Both relative reflectance were normalized at V-band.

Table 1. Observatories and Instruments

Observatory Name	Longitude	Latitude	Elevation (m)	Telescope Diameter (m)	CCD	Field of View
Vatican	109°53′31.25”W	32°42′04.69”N	3191	1.8	VATT2K	$6.8' \times 6.8'$
Kiso	137°37′42.2”E	35°47′38.7”N	1130	1.05	2kCCD	$50' \times 50'$
FUE*	130°35′44.7”E	33°48′45.3”N	70	0.40	SBIG ST6	$5.75' \times 4.36'$

*Fukuoka University of Education

Table 2. Aspect data of observations

Date (UT)	RA	DEC	r (AU)	Δ (AU)	Phase angle (deg)	sky motion (”/min)	Obs.
(832) Karin							
2003-07-31.65	22 24 28.68	-08 23 42.1	2.697	1.752	9.80	0.38	FUE
2003-08-01.64	22 23 54.61	-08 26 33.0	2.697	1.746	9.42	0.39	FUE
2003-08-02.69	22 23 17.37	-08 29 40.6	2.696	1.740	9.02	0.41	FUE
2003-08-03.73	22 22 39.55	-08 32 52.6	2.695	1.734	8.62	0.42	FUE
2003-08-06.76	22 20 42.62	-08 42 53.4	2.694	1.718	7.42	0.45	FUE
2003-08-09.07	22 18 41.33	-08 53 25.8	2.692	1.705	6.22	0.48	FUE
2003-08-22.64	22 08 43.42	-09 46 32.8	2.684	1.673	0.85	0.55	FUE
2003-08-23.64	22 07 55.14	-09 50 53.7	2.684	1.673	0.61	0.55	FUE
2003-09-03.63	21 59 11.55	-10 38 31.7	2.678	1.684	4.70	0.49	FUE
2003-09-04.63	21 58 26.40	-10 42 40.8	2.677	1.687	5.13	0.48	FUE
2003-09-05.61	21 57 43.07	-10 46 40.6	2.677	1.690	5.54	0.47	FUE
2003-09-05.61	21 57 43.07	-10 46 40.6	2.677	1.690	5.54	0.47	Kiso
2003-09-06.61	21 57 43.07	-10 46 40.6	2.677	1.690	5.54	0.47	Kiso
2003-09-26.19	21 46 09.10	-11 53 00.2	2.666	1.803	13.36	0.24	VATT*
2003-09-27.19	21 45 49.21	-11 55 05.7	2.666	1.811	13.68	0.22	VATT*
2003-09-28.17	21 45 30.91	-11 57 03.3	2.665	1.819	13.99	0.21	VATT*
2003-09-29.17	21 45 13.56	-11 58 56.7	2.665	1.827	14.30	0.19	VATT*

Observatory Code: VATT - Vatican; Kiso - Kiso Observatory; FUE - Fukuoka University of Education. *BVRI-color observations were performed.

UT start	filter	T_{exp} (sec)	Colors
2003 Sep 26			
3.421	R	40	
3.448	R	40	
3.476	I	40	$I-R=$
3.502	I	40	-0.382
3.531	R	40	
3.557	R	40	
3.586	V	60	$V-R=$
3.630	V	60	0.434
3.669	V	60	
3.709	R	40	
3.734	R	40	
3.762	R	40	
3.789	I	40	$I-R=$
3.814	I	40	-0.374
3.840	R	40	
3.865	R	40	
3.906	B	120	$B-R=$
3.956	B	120	1.241
4.023	R	40	
4.048	R	40	
4.313	R	40	
4.344	R	40	
4.370	B	120	$B-R=$
4.418	B	120	1.234
4.466	R	40	
4.491	R	40	
4.517	I	40	$I-R=$
4.543	I	40	-0.363
4.569	R	40	
4.595	R	40	
4.624	V	60	$V-R=$
4.655	V	60	0.457
4.689	R	40	
4.714	R	40	

Table 3. (Continued)

4.743	I	40	$I-R=$
4.768	I	40	-0.373
4.795	R	40	
4.820	R	40	
4.945	R	40	
4.981	R	40	
5.213	R	40	
5.252	R	40	
5.292	B	120	$B-R=$
5.340	B	120	1.251
5.390	R	40	
5.418	R	40	
5.444	I	40	$I-R=$
5.468	I	40	-0.391
5.494	R	40	
5.519	R	40	
5.545	V	60	$V-R=$
5.576	V	60	0.459
5.608	R	40	
5.632	R	40	
5.714	R	40	
5.739	R	40	
5.766	B	120	$B-R=$
5.813	B	120	1.223
5.866	R	40	
5.891	R	40	
2003 Sep 27			
2.628	R	40	
2.658	R	40	
2.689	B	120	$B-R=$
2.737	B	120	1.220
2.790	R	40	
2.815	R	40	
2.844	V	60	$V-R=$
2.874	V	60	0.449
2.906	R	40	
2.933	R	40	

Table 3. (Continued)

2.972	I	40	$I-R=$
2.997	I	40	-0.378
3.023	R	40	
3.048	R	40	
3.075	B	120	$B-R=$
3.128	B	120	1.203
3.177	R	40	
3.201	R	40	
3.228	V	60	$V-R=$
3.259	V	60	0.460
3.296	R	40	
3.325	R	40	
5.764	R	40	
5.801	R	40	
5.827	R	40	
5.855	B	120	$B-R=$
5.902	B	120	1.229
5.953	R	40	
5.978	R	40	
6.005	V	60	$V-R=$
6.035	V	60	0.455
6.071	R	40	
6.095	R	40	
6.124	I	40	$I-R=$
6.148	I	40	-0.462
6.174	R	40	
6.200	R	40	
6.231	B	120	$B-R=$
6.278	B	120	1.210
6.328	R	40	
6.357	R	40	
6.384	V	60	$V-R=$
6.414	V	60	0.453
6.451	R	40	
6.478	R	40	
2003 Sep 28			
2.136	R	40	

Table 3. (Continued)

2.191	R	40	
2.227	V	60	$V-R=$
2.257	V	60	0.458
2.290	R	40	
2.316	R	40	
2.346	I	40	$I-R=$
2.370	I	40	-0.386
2.396	R	40	
2.421	R	40	
2.447	B	120	$B-R=$
2.493	B	120	1.228
2.548	R	40	
2.573	R	40	
2.599	V	60	$V-R=$
2.629	V	60	0.451
2.664	R	40	
2.688	R	40	
2.716	I	40	$I-R=$
2.742	I	40	-0.384
2.767	R	40	
2.792	R	40	
5.563	R	40	
5.594	R	40	
5.621	V	60	$V-R=$
5.652	V	60	0.451
5.685	R	40	
5.709	R	40	
5.741	I	40	$I-R=$
5.766	I	40	-0.385
5.792	R	40	
5.817	R	40	
5.846	B	120	$B-R=$
5.893	B	120	1.254
5.942	R	40	
5.966	R	40	
5.997	V	60	$V-R=$
6.027	V	60	0.457

Table 3. (Continued)

6.061	R	40	
6.086	R	40	
6.111	I	40	$I-R=$
6.136	I	40	-0.930
6.162	R	40	
6.187	R	40	
2003 Sep 29			
2.276	R	40	
2.316	R	40	
2.349	I	40	$I-R=$
2.374	I	40	-0.340
2.404	R	40	
2.429	R	40	
2.456	B	120	$B-R=$
2.502	B	120	1.254
2.564	R	40	
2.588	R	40	
2.616	V	60	$V-R=$
2.646	V	60	0.443
2.679	R	40	
2.703	R	40	
2.731	B	120	$B-R=$
2.785	B	120	1.234
2.834	R	40	
2.859	R	40	
2.886	I	40	$I-R=$
2.911	I	40	-0.350
2.939	R	40	
2.964	R	40	
5.287	R	40	
5.313	R	40	
5.339	V	60	$V-R=$
5.369	V	60	0.452
5.404	R	40	
5.428	R	40	
5.453	R	40	
5.479	I	40	$I-R=$

Table 3. (Continued)

5.504	I	40	-0.349
5.529	R	40	
5.554	R	40	
5.581	B	120	$B-R=$
5.628	B	120	1.244
5.677	R	40	
5.701	R	40	
5.728	V	60	$V-R=$
5.758	V	60	0.452
5.789	R	40	
5.814	R	40	
5.840	I	40	$I-R=$
5.864	I	40	-0.354
5.889	R	40	
5.913	R	40	